Iterative adaptive signal predistortion for satellite communications

Nicolas Alibert, Karine Amis Cavalec, Charlotte Langlais, Damien Castelain

Iterative adaptive signal predistortion for satellite communications

Nicolas Alibert*†, Karine Amis†, Charlotte Langlais†, Damien Castelain*
*Wireless Communications Systems Department, Mitsubishi Electric R&D Centre Europe,
1 allée de Beaulieu, CS 10806, 35708 Rennes Cedex 7, France
Email: {n.alibert,d.castelain}@fr.merce.mee.com
† IMT Atlantique, Lab-STICC,UBL, F-29238 Brest, France
Email: {karine.amis,charlotte.langlais}@imt-atlantique.fr

***Abstract*—The expected increase of data rates in future satellite communications (DVB-S2X) will require higher-order modulations and sharper roll-off, which makes the transmission more sensitive to non-linear interference due to on-board amplifiers. One solution is the predistortion of the signal that is carried out at the transmitter. Iterative predistortion based on the contraction mapping theorem has shown to be a good solution to mitigate the effects of nonlinearities but suffers from convergence depending on the chosen norm. In this paper, we propose to adapt the method with a feedback from the channel to ensure the convergence with the best linearization performance for a given number of iterations. We compare both schemes according to different figures of merit (adjacent channel interference factor, total degradation and normalized mean square error).**

I. Introduction

The need for higher data rates in satellite communications has pushed to develop the DVB-S2X [1], which introduces more spectrally-efficient constellations and sharper roll-off. However, high-order constellations are more sensitive to non-linearities generated by the on-board amplifier and the sharper roll-of increases the peak-to-average ratio (PAPR), which induces more distortion. The compensation of non-linearities is, then, a key point for higher satellite throughput [2].

The mitigation of non-linear distortion can either be done at the transmitter with predistortion [2]–[8] or at the receiver with equalization [9]. In the literature, the predistortion techniques are separated into two categories, the data predistortion, which operates at symbol rate [8], [10], and the signal predistortion which operates at a higher sample rate after the pulse shaping filter [2]–[7].

One class of signal predistortion techniques relies on the application of the contraction mapping theorem, which aims to linearize the non-linear channel with [4]–[6] or without memory [7]. These techniques use an iterative optimization algorithm. The optimization error is defined from the desired signal at the non-linear system output.

Nonetheless, the convergence depends on the chosen norm and often only upper bounds can be computed [4]. A method using a fixed damping factor in order to ensure the convergence has been proposed in [7]. However, this gain has to be tuned empirically and it has an impact on linearization performance. When the convergence conditions are unfulfilled, using the structure with a judiciously chosen number of stages can make the equivalent channel more linear [6].

In this paper, we focus on a signal predistortion scheme based on the contraction mapping theorem in the context of satellite communications [3]. Then, to ensure the best linearization performance, for a given number of stages, and convergence, we modify the latter structure by adding extra parameters. Moreover, to avoid empirical tuning of these parameters, we derive an adaptation process based on a feedback from the channel. Finally, we compare adaptive and non-adaptive schemes in terms of adjacent channel interference (ACI), normalized mean square error (NMSE) and total degradation (TD). The paper is organized as follows. Section II describes the system model. The reference iterative signal predistortion technique based on the contraction mapping theorem is described in Section III. The proposed iterative adaptive signal predistortion is described in Section IV. The comparison of both schemes in terms of NMSE, ACI, TD is carried out in Section V. Finally, Section VI concludes the paper.

II. System model

This paper focuses on single-carrier satellite communications. The single-carrier-per-transponder scenario allows to operate closer to the saturation, which improves the amplifier efficiency [11].

The satellite transponder is composed of three elements: the input multiplexer (IMUX), the non-linear high power amplifier (HPA) and the output multiplexer (OMUX). The cascade of those three elements behaves as a non-linear channel with memory [12], which is the main source of impairment.

The uplink channel, from the transmitter to the satellite transponder, is considered to be noise-free. On the downlink, from the satellite transponder to the receiver, the signal is affected by additive white Gaussian noise (AWGN) and adjacent carrier interference (ACI).

We also assume that the overall impulse response $h_{TX} * g_{RX}$, where h_{TX} and g_{RX} are the transmitter and the receiver filters respectively, satisfies the Nyquist intersymbol interference (ISI) criterion. The up-sampled transmitted signal vector, at the output of the modulator, associated to the l-th frame is denoted by $\boldsymbol{X}(l)$ and is defined by

$\boldsymbol{X}(l) = \left[x_{0+lM}, x_{1+lM}, \ldots, x_{M-1+lM}\right]^T$, where $x_{i+lM}, i \in \{0, \ldots, M-1\}$ is the i-th sample of the l-th sampled signal frame. M is the data symbol frame length times the oversampling factor.

The discrete impulse response of IMUX filter is described by an $M \times M$ Toeplitz matrix $\boldsymbol{H}$ generated by the vector $\boldsymbol{h} = [h_{-L} \cdots h_0 \cdots h_L]^T$ of length $(2L+1)$.

Likewise, the discrete impulse response of OMUX filter is described by the vector $\boldsymbol{g} = [g_{-P} \cdots g_0 \cdots g_P]^T$ of length $(2P+1)$ and is associated to the $M \times M$ matrix $\boldsymbol{G}$.

The non-linear HPA is represented by the function $f(.)$. Given $\boldsymbol{Z} = [z_0 \ \cdots \ z_{M-1}]^T$, the notation $f(\boldsymbol{Z})$ stands for a vector of length M, whose i-th component equals $f(z_i)$. Similarly, we define the function $\mathcal{R}(.)$ which represents the nonlinear channel with memory.

III. Signal predistortion based on the contraction mapping theorem

Iterative predistortion technique based on the contraction mapping theorem has been a solution proposed to linearize an non-linear channel with memory [3]–[6] or without memory [7]. The predistortion problem can be formulated as follows:

$$\mathcal{R}\{\bar{\boldsymbol{X}}(l)\} = \zeta \boldsymbol{X}(l), \tag{1}$$

where $\bar{\boldsymbol{X}}(l)$ is the predistorted signal ($M \times 1$ vector), $\boldsymbol{X}(l)$ is the desired signal at the output of the non-linear channel ($M \times 1$ vector), $\mathcal{R}$ is the non-linear channel with memory, which, in our case, corresponds to the satellite transponder and ζ defines the desired ideal gain at the output of the non-linear channel.

The problem can be reformulated as a fixed-point problem, either by inverting the linear part of $\mathcal{R}$ as in [4], [5] or by adding on both sides $(I-\mathcal{R})\{\bar{\boldsymbol{X}}(l)\}$ as in [6]. The latter solution avoids a computationally expensive inversion of the linear part of the channel.

The mathematical formulation of the predistortion problem as fixed-point one is then:

$$(I-\mathcal{R})\{\bar{\boldsymbol{X}}(l)\} + \zeta \boldsymbol{X}(l) = \bar{\boldsymbol{X}}(l). \tag{2}$$

If the conditions for the contraction mapping are met for the operator $\mathcal{T}\{.\} = (I-\mathcal{R})\{.\} + \zeta \boldsymbol{X}(l)$, the solution is unique and it can be iteratively reached by using:

$$\bar{\boldsymbol{X}}^{(k+1)}(l) = \mathcal{T}\{\bar{\boldsymbol{X}}^{(k)}(l)\}, \tag{3}$$

where k is the stage number of the iterative process. The conditions for the operator $\mathcal{T}\{.\}$ to be a contraction mapping, when the non-linear system can be described as a Volterra model, are given in [4], [6]. However, the verification of the conditions might be cumbersome as they depend on the chosen norm. Often, the conditions cannot be computed and upper bounds are used [4]. On the other hand, if the conditions are unfulfilled, performing few iterations might improve the linearity of the equivalent channel [6]. Moreover, an appropriate constant γ can be introduced to make $\mathcal{T}\{.\}$ a contraction mapping [7]. The recursion equation (3) then becomes:

$$\bar{\boldsymbol{X}}^{(k+1)}(l) = \bar{\boldsymbol{X}}^{(k)}(l) + \gamma\left(\zeta \boldsymbol{X}(l) - \mathcal{R}\{\bar{\boldsymbol{X}}^{(k)}(l)\}\right). \tag{4}$$

γ has to be tuned empirically for each channel $\mathcal{R}$. In some cases, it should be made decreasing with the iterations, which requires further empirical tuning [13].

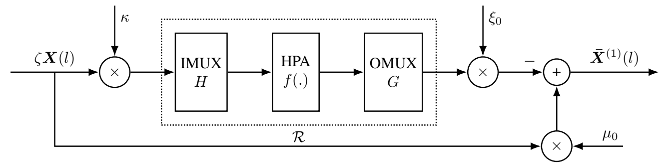

Fig. 1. First stage of the proposed iterative adaptive signal predistortion scheme.

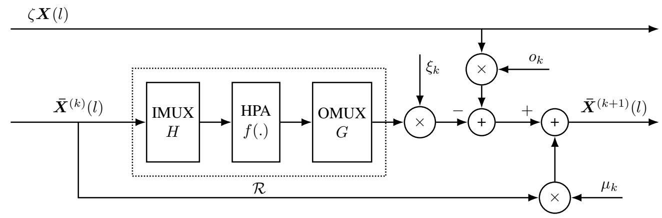

Fig. 2. k-th stage ($k \geq 1$) of the proposed iterative adaptive signal predistortion scheme.

IV. Proposed iterative adaptive signal predistortion

The proposed iterative adaptive signal predistortion scheme is based on the previous formulation of the fixed-point problem given by (1). In order to circumvent the issue of empirical tuning of parameter, we introduce gains that can be adapted with a feedback from the channel. Those extra gains are used to ensure the best performance after a given number of iterations and convergence when the conditions of the contraction mapping theorem are unfulfilled. Like the direct learning architecture [14], [15], the predistortion scheme is twice-adaptive. It requires the channel identification as preliminary step, then the stages are adapted. In this paper, we consider that the channel model $\mathcal{R}$ is known.

A. Iterative predistortion process

Based on (4), we propose a novel formulation of the iterative signal predistortion scheme such that the predistorted signal at stage k is computed as follows:

$$\bar{\boldsymbol{X}}^{(k+1)}(l) = \mu_k \bar{\boldsymbol{X}}^{(k)}(l) - \boldsymbol{e}_k(l), \tag{5}$$

with $\boldsymbol{e}_k(l)$ the update error defined by

$$\boldsymbol{e}_k(l) = \xi_k \mathcal{R}\{\bar{\boldsymbol{X}}^{(k)}(l)\} - o_k \zeta \boldsymbol{X}(l), \quad k \geq 1. \tag{6}$$

Thus, at the k-th stage ($k \geq 1$), the predistorted signal $\bar{\boldsymbol{X}}^{(k+1)}(l)$ is computed as the sum between two terms. The first one is the predistorted signal $\bar{\boldsymbol{X}}^{(k)}(l)$ computed at previous stage. Its contribution to the definition of $\bar{\boldsymbol{X}}^{(k+1)}(l)$ is weighted by the feedforward gain denoted by μ_k. The second one, the update signal $\boldsymbol{e}_k(l)$ is the error between the output of the channel model, with the predistorted signal equal to $\bar{\boldsymbol{X}}^{(k)}(l)$ weighted by ξ_k, and the reference signal $\boldsymbol{X}(l)$, weighted by o_k. Instead of having one parameter weighting the error, we have introduced an extra degree of freedom by using two separate gains. The post model gain, denoted by ξ_k, enables to adjust the level at the output of the channel model. The reference gain, denoted by o_k, aims at controlling the contribution of the reference signal. The combination of the three gains (o_k, μ_k, ξ_k) allows the process to select the amplifier's operating point and blend the three components to generate the output of the stage $\bar{\boldsymbol{X}}^{(k+1)}(l)$.

At $k = 0$, the process is initialized with $\bar{\boldsymbol{X}}^{(0)}(l) = \zeta \boldsymbol{X}(l)$. Equation (5) can be simplified since the initialization signal and the reference signal are equal in this case. The first iteration is then expressed as follows:

$$\bar{\boldsymbol{X}}^{(1)}(l) = \mu_0 \zeta \boldsymbol{X}(l) - \xi_0 \mathcal{R}\{\kappa \zeta \boldsymbol{X}(l)\}, \quad k = 0. \tag{7}$$

An additional pre-model gain κ is introduced to adjust the operating point of the model depending on the initial signal amplitude (which can be either too low or high). The feedforward gain μ_0 controls the part of the initialization for the next stage and the computation of the error.

Figure 1 and 2 illustrate first ($k = 0$) and intermediate ($k \geq 1$) stages respectively.

B. Adaptation process

The adaptation process consists in defining the gains $(\kappa, o_k, \mu_k, \xi_k)$ through an iterative process that computes $(\kappa_n, o_{k,n}, \mu_{k,n}, \xi_{k,n})$. Subscript k and n refer to the predistortion stage and to the adaptation process iteration, respectively.

The k-th predistortion output is computed once the parameter adaptation process has converged or when the iteration number n has reached its maximum value (fixed to N). The stages are adapted one after the other until the pre-defined number of stages K is reached. This procedure allows to avoid the problem of vanishing or exploding gradient for the early stages since the value of the gradient depends on gain values of the following stage. Once the adaptation process of the k-th stage is over, the gains $(\kappa_n,\ o_{k,n},\ \mu_{k,n},\ \xi_{k,n})$ are definitively fixed to their convergence state values $(\kappa,\ o_k,\ \mu_k,\ \xi_k) = (\kappa_N,\ o_{k,N-1},\ \mu_{k,N-1},\ \xi_{k,N-1}))$.

Let us denote by $\boldsymbol{Y}(p)$ the p-th nonlinear channel output ($p = kN + n$) vector of length M. Taking into account the delay D introduced by the channel, the predistorted signal $\bar{\boldsymbol{X}}(p - D)$ is computed so as to minimize the following cost function:

$$J(p) = \boldsymbol{E}^{\dagger}(p)\boldsymbol{E}(p) \tag{8}$$

where the error vector $\boldsymbol{E}(p)$ is equal to $\zeta \boldsymbol{X}(p - D) - \boldsymbol{Y}(p)$.

During the k-th stage of the adaptation process, the output of the channel model at the p-th iteration is expressed as:

$$\boldsymbol{Y}(p) = \mathcal{R}\{\bar{\boldsymbol{X}}_t^{(k+1)}(p)\}, \tag{9}$$

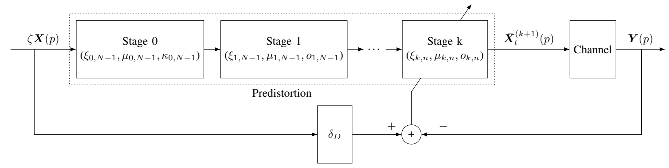

Fig. 3. Adaptation of the k-th stage.

where the training predistorted signal $\bar{\boldsymbol{X}}_t^{(k+1)}(p)$ at iteration p is computed as follows:

$$\bar{\boldsymbol{X}}_t^{(k+1)}(p) = \begin{cases} \mu_{0,n}\boldsymbol{X}(p) - \xi_{0,n}\mathcal{R}\{\kappa_n \zeta \boldsymbol{X}(p)\}, & k = 0 \\ \begin{bmatrix} \mu_{k,n}\bar{\boldsymbol{X}}^{(k)}(p) + o_{k,n}\zeta \boldsymbol{X}(p) \\ -\xi_{k,n}\mathcal{R}\{\bar{\boldsymbol{X}}^{(k)}(p\} \end{bmatrix}, & k \geq 1 \end{cases} \tag{10}$$

with $\bar{\boldsymbol{X}}^{(k)}(p)$ computed by (5) or (7) with the gains fixed to $(\kappa,\ o_k,\ \mu_k,\ \xi_k)$ obtained after the adaptation process of k-th stage.

Figure 3 illustrates the process. In the latter, δ_D denotes the Dirac function delayed by D, which is the delay induced by the channel.

The gains are initialized as follows:

- $\kappa_0 = 1$
- $\mu_{k,0} = 1, \forall k$
- $\xi_{k,0} = 0, \forall k$
- $o_{k,0} = 0, \forall k \geq 1$

We suppose that all the gains are real. Given the k-th predistortion stage output $\bar{\boldsymbol{X}}^{(k)}(p)$, the gradient of the cost function for the feedforward parameter μ_k is:

$$\begin{aligned} \frac{\partial J(p)}{\partial \mu_{k,n}} = &- 2\Re\left(\boldsymbol{E}^{\dagger}(p)\left[\frac{\partial \boldsymbol{Y}(p)}{\partial \bar{\boldsymbol{X}}^{(k+1)}(p-D)}\bar{\boldsymbol{X}}^{(k)}(p-D)\right.\right. \\ &\left.\left. + \frac{\partial \boldsymbol{Y}(p)}{\partial\left(\bar{\boldsymbol{X}}^{(k+1)}(p-D)\right)^*}\left(\bar{\boldsymbol{X}}^{(k)}(p-D)\right)^*\right]\right). \end{aligned} \tag{11}$$

Then, the feedforward parameter is updated by applying the LMS algorithm, as follows:

$$\mu_{k,n+1} = \mu_{k,n} - c_{\mu}\frac{\partial J(p)}{\partial \mu_{k,n}}, \tag{12}$$

with c_{μ} a step-size. The other gains $o_{k,n}$, $\xi_{k,n}$ and κ_n are updated in a similar way with the following gradients:

$$\begin{aligned} \frac{\partial J(p)}{\partial o_{k,n}} = &- 2\Re\left(\boldsymbol{E}^{\dagger}(p)\left[\frac{\partial \boldsymbol{Y}(p)}{\partial \bar{\boldsymbol{X}}^{(k+1)}(p-D)}\boldsymbol{X}(p-D)\right.\right. \\ &\left.\left. + \frac{\partial \boldsymbol{Y}(p)}{\partial\left(\bar{\boldsymbol{X}}_t^{(k+1)}(p-D)\right)^*}\left(\boldsymbol{X}(p-D)\right)^*\right]\right), \end{aligned} \tag{13}$$

$$\frac{\partial J(p)}{\partial \xi_{k,n}} = 2\Re\left(\boldsymbol{E}^{\dagger}(p)\left[\frac{\partial \boldsymbol{Y}(p)}{\partial \bar{\boldsymbol{X}}_t^{(k+1)}(p-D)}\mathcal{R}\{\bar{\boldsymbol{X}}^{(k)}(p-D)\}\right.\right.$$
$$\left.\left.+\frac{\partial \boldsymbol{Y}(p)}{\partial\left(\bar{\boldsymbol{X}}_t^{(k+1)}(p-D)\right)^*}\left(\mathcal{R}\{\bar{\boldsymbol{X}}^{(k)}(p-D)\}\right)^*\right]\right), \tag{14}$$

$$\frac{\partial J(p)}{\partial \kappa_n} = 2\Re\left(\xi_0\boldsymbol{E}^{\dagger}(p)\left[\frac{\partial \boldsymbol{Y}(p)}{\partial \bar{\boldsymbol{X}}^{(1)}(p-D)}\widehat{X}^{(k)}(p-D)\right.\right.$$
$$\left.\left.+\frac{\partial \boldsymbol{Y}(p)}{\partial\left(\bar{\boldsymbol{X}}^{(1)}(p-D)\right)^*}\left(\widehat{X}^{(k)}(p-D)\right)^*\right]\right). \tag{15}$$

with:

$$\widehat{X}^{(k)}(p) = \left(\frac{\partial \mathcal{R}}{\partial \boldsymbol{Z}}\left(\kappa_n\boldsymbol{H}^T\bar{\boldsymbol{X}}^{(k)}(p)\right)\boldsymbol{H}^T\bar{\boldsymbol{X}}^{(k)}(p)\right.$$
$$\left.+\frac{\partial \mathcal{R}}{\partial \boldsymbol{Z}^*}\left(\kappa_n\boldsymbol{H}^T\bar{\boldsymbol{X}}^{(k)}(p)\right)\left(\boldsymbol{H}^T\bar{\boldsymbol{X}}^{(k)}(p)\right)^*\right), \tag{16}$$

V. Performance evaluation

In this section, we compare the performance of the iterative signal predistortion based on the contraction mapping used as reference and the proposed iterative adaptive signal predistortion through Monte Carlo simulations. The transmitter and receiver filter are square-root raised cosine (SRRC) filters with a 5% roll-off. The IMUX and OMUX characteristics are the one defined in the DVB-S2 [16]. The symbol rate is set to 38 MBd. The model used for the traveling wave tube amplifier is defined in [17]. The amplitude-to-amplitude modulation is expressed as:

$$A(\rho) = \alpha_a \frac{\rho}{1+\beta_a\rho^2} \tag{17}$$

and the amplitude-to-phase modulation is given by:

$$\Phi(\rho) = \alpha_\phi \frac{\rho(t)^2}{1+\beta_\phi\rho^2} \tag{18}$$

with ρ the modulated envelope. The four parameters are set as follows: $\alpha_a = 1, \beta_a = 2, \alpha_\phi = 1, \beta_\phi = 2$.

The interferers are delayed and time-shifted versions of the output of the OMUX filter located at 40 MHz on both sides of the carrier of interest [18]. In the simulations, the step-size γ for the iterative signal predistortion is adjusted for an input back-off (IBO) of 13dB and we take $c_\mu = c_\xi = c_o = 10^{-3}$ and $c_\kappa = 10^{-5}$. The training is done with N =2000 frames of 128 symbols for each stage.

A. Figures of merit

The total degradation (TD) in dB, for a given bit error rate (BER), is expressed as:

$$TD = OBO + \left.\frac{E_b}{N_0}\right|_{NL} - \left.\frac{E_b}{N_0}\right|_{AWGN} \quad \text{[dB]}. \tag{19}$$

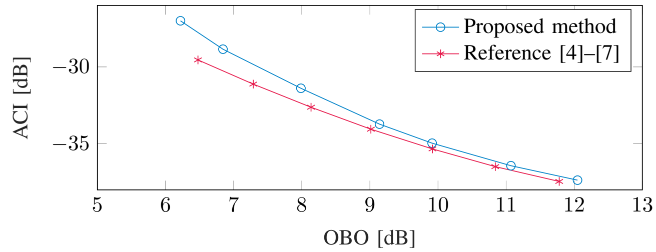

Fig. 4. ACI at the output of the matched filter versus the OBO.

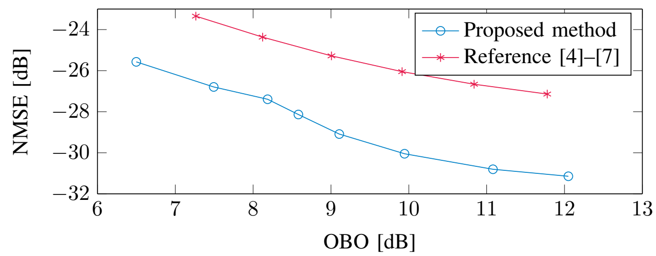

Fig. 5. NMSE versus the OBO.

The quality of the compensation of the nonlinearities is measured by the difference of signal-to-interference-plus-noise ratio (SINR) between the nonlinear case and the AWGN case, respectively denoted: $\left.\frac{E_b}{N_0}\right|_{NL}$ and $\left.\frac{E_b}{N_0}\right|_{AWGN}$. The output back-off ($OBO$) measures the difference between the maximum power of the amplifier output and the mean power of the receive filter output.

The in-band distortion is measured with the $NMSE$ at the receiver given by:

$$NMSE = 10\log\left(\mathrm{E}\left[\frac{||\hat{d}-d||^2}{||d||^2}\right]\right) \quad \text{[dB]}, \tag{20}$$

where E is the mathematical expectation, $\hat{d}$ and d are respectively, the gain and phase corrected sequence of symbols at the receiver output *without ACI* and the desired sequence of symbols.

We measure the interference at the output of the receiver filter g_{RX} by the parameter denoted by ACI and equal to:

$$ACI = 10\log\left(\mathrm{E}\left[\frac{\int|(y_{AC} * g_{RX})(t)|^2\mathrm{d}t}{\int|(y * g_{RX})(t)|^2\mathrm{d}t}\right]\right) \quad \text{[dB]}, \tag{21}$$

with y_{AC} and y, respectively the interferers and the carrier of interest at the output of the satellite transponder. The ACI factor quantifies the spillage due to the spectral regrowth of adjacent carriers.

The quality of the adaptation is measured by the normalized mean square error defined as follows:

$$AMSE = 10\log\left(\mathrm{E}\left[\frac{||\boldsymbol{Y}(p)-\zeta\boldsymbol{X}(p-D)||^2}{||\zeta\boldsymbol{X}(p-D)||^2}\right]\right) \quad \text{[dB]}, \tag{22}$$

B. Results

The ACI factor as a function of OBO is given in Figure 4 for both the iterative predistortion based on the fixed point and

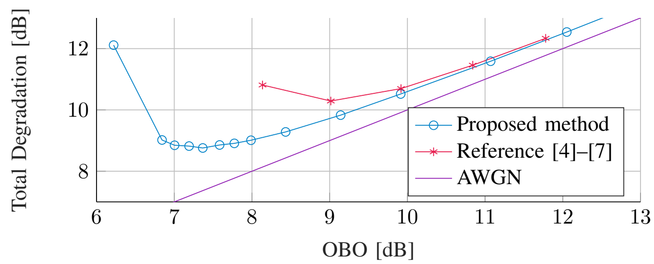

Fig. 6. Total degradation with ACI for a target BER of 10^{-4} for the reference method and the proposed method for 10 iterations.

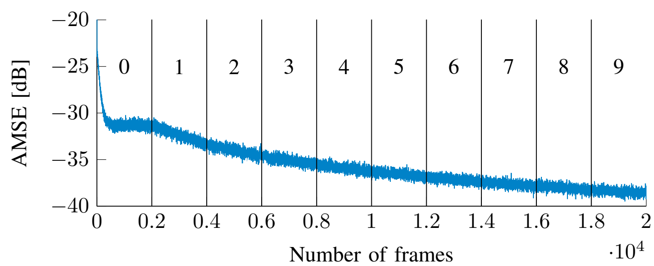

Fig. 7. AMSE versus number of frames p.

the proposed iterative adaptive method. As OBO increases, the HPA reponse is more linear and therefore the ACI decreases. The reference method outperforms the proposed one by 2.5 dB in the worst case.

On the other hand, concerning the NMSE, which relates to the in-band distortion, the trend is reversed. The proposed adaptive method outperforms the reference method, up to 4dB.

The total degradation (TD) *with* ACI as a function of OBO is plotted in Figure 6. The optimal point which minimizes the TD (the lowest along the vertical axis) for the proposed method is better by 1.55dB.

Figure 7 illustrates the AMSE defined in (22) during the adaptation process as a function of the number of frames p. The upper number mentions the stage under adaptation. When a black vertical line is met, the gains of the current stage are set to the values reached at the end of the adaptive process and the adaptation of the following stage begins. At first stage output, the adaptation has reached a plateau and the addition of a new stage allows to further decrease the error. The continuity of the AMSE is ensured by the initialization parameter chosen for each stage.

VI. Conclusion

In this paper, we proposed an adaptive process for the iterative signal predistortion scheme based on the contraction mapping theorem. The proposed algorithm circumvents the difficult calculus of convergence conditions and ensures an improvement of linearization whenever the conditions of the contraction mapping theorem are unfulfilled. Moreover, it avoids empirical tuning of parameters. To do so, three gains were introduced and adapted by a LMS algorithm stage by stage. The issue of exploding or vanishing gradient is avoided by adding the stage one after the other. Monte-Carlo simulations show that, thanks to the gain adaptation, the iterative adaptive signal predistortion outperforms the non-adaptive one in terms of NMSE and Total Degradation, with a gain of 1.55 dB for the latter. Further works will sudy the impact of channel mismatch on the performance of the proposed method.

References

[1] European Telecommunications Standards Institute, "Digital Video Broadcasting (DVB); Second generation framing structure, channel coding and modulation systems for Broadcasting, Interactive Services, News Gathering and other broadband satellite applications; Part 2: DVB-S2 Extensions (DVB-S2X)," 2015.

[2] B. F. Beidas, "Adaptive Digital Signal Predistortion for Nonlinear Communication Systems Using Successive Methods," *IEEE Trans. Commun.*, vol. 64, no. 5, pp. 2166–2175, may 2016.

[3] N. Alibert, K. Amis, C. Langlais, and D. Castelain, "Signal predistortion scheme based on the contraction mapping theorem," in *GRETSI 2017 26ème Colloq. du Group. Rech. en Trait. du Signal des Images*, Juan-Les-Pins, France, 2017.

[4] R. Nowak and B. Van Veen, "Volterra filter equalization: a fixed point approach," *IEEE Trans. Signal Process.*, vol. 45, no. 2, pp. 377–388, feb 1997.

[5] E. Aschbacher, M. Steinmair, and M. Rupp, "Iterative linearization methods suited for digital pre-distortion of power amplifiers," *Conf. Rec. Thirty-Eighth Asilomar Conf. Signals, Syst. Comput. 2004.*, vol. 2, no. 4, pp. 5–9, 2004.

[6] M. Hotz and C. Vogel, "Linearization of time-varying nonlinear systems using a modified linear iterative method," *IEEE Trans. Signal Process.*, vol. 62, no. 10, pp. 2566–2579, 2014.

[7] M.-C. Kim, Y. Shin, and S. Im, "Compensation of nonlinear distortion using a predistorter based on the fixed point approach in OFDM systems," *VTC '98. 48th IEEE Veh. Technol. Conf.*, vol. 3, pp. 2145–2149, 1998.

[8] T. Deleu, M. Dervin, K. Kasai, and F. Horlin, "Iterative Predistortion of the nonlinear satellite channel," *IEEE Trans. Commun.*, vol. 62, no. 8, pp. 2916–2926, aug 2014.

[9] S. Benedetto and E. Biglieri, "Nonlinear Equalization of Digital Satellite Channels," *IEEE J. Sel. Areas Commun.*, vol. 1, no. 1, pp. 57–62, 1983.

[10] G. Karam and H. Sari, "A data predistortion technique with memory for QAM radio systems," *IEEE Trans. Commun.*, vol. 39, no. 2, pp. 336–344, 1991.

[11] A. Ugolini, A. Modenini, G. Colavolpe, V. Mignone, and A. Morello, "Advanced techniques for spectrally efficient DVB-S2X systems," *Int. J. Satell. Commun. Netw.*, vol. 34, no. 5, pp. 609–623, sep 2016.

[12] S. Benedetto, E. Biglieri, and R. Daffara, "Modeling and Performance Evaluation of Nonlinear Satellite Links-A Volterra Series Approach," *Aerosp. Electron. Syst. IEEE Trans.*, vol. AES-15, no. 4, pp. 494–507, 1979.

[13] E. Zeidler, *Nonlinear functional analysis and its application I: Fixed-Point Theorems*, Springer-Verlag New York, 1985.

[14] R. Piazza, M. Bhavani Shankar, and B. Ottersten, "Generalized direct predistortion with adaptive crest factor reduction control," in *2015 IEEE Int. Conf. Acoust. Speech Signal Process.* apr 2015, number 1, pp. 3242–3246, IEEE.

[15] D. Zhou and V. E. DeBrunner, "Novel adaptive nonlinear predistorters based on the direct learning algorithm," *IEEE Trans. Signal Process.*, vol. 55, no. 1, pp. 120–133, 2007.

[16] European Telecommunications Standards Institute, "Digital Video Broadcasting (DVB); Second generation framing structure, channel coding and modulation systems for Broadcasting, Interactive Services, News Gathering and other broadband satellite applications; Part 1: DVB-S2," 2014.

[17] A. A. M. Saleh, "Frequency-Independent and Frequency-Dependent Nonlinear Models of TWT Amplifiers," *IEEE Trans. Commun.*, vol. 29, no. 11, pp. 1715–1720, 1981.

[18] N. Alibert, K. Amis, C. Langlais, and D. Castelain, "Comparison of signal predistortion schemes based on the contraction mapping for satellite communications with channel identification," in *25th Int. Conf. Telecommun.*, 2018.